

Physical Principles of Nuclear Magnetic Resonance and Applications

David Stephen, Tao Fang and Jordan Wilson

(Dated: November 25, 2016)

I. Introduction

In this paper we review the phenomenon of nuclear magnetic resonance (NMR). We employ a proper quantum mechanical treatment along with the usual semi-classical picture to explain underlying principles and experimental methods. We also describe mechanisms of relaxation in NMR systems. The paper concludes with examples of modern uses of NMR.

II. Magnetic Resonance - Basic Theory

Nuclear magnetic resonance was first observed by Rabi in 1938 (Rabi *et al.*, 1938). He started with a simple Stern-Gerlach experiment consisting of nuclei fired through a strong inhomogeneous magnetic field. Depending on their nuclear spin, the nuclei are deflected by the field towards various detectors. Rabi introduced the modification of a wire coil midway through the field which was able to create a perpendicular magnetic field oscillating at radio frequencies (RF). He noticed that, when the strength of the static field was properly tuned, it would result in a sudden dip in beam intensity at a certain detector. Rabi correctly deduced that the oscillating field had induced transitions in the spin states of the nuclei, causing them to be deflected along a different path by the Stern-Gerlach apparatus. By identifying this point of resonance, Rabi was able to deduce the nuclear magnetic moment.

The results of Rabi's experiment can be explained with basic quantum mechanics. In an external magnetic field $\vec{H}_0 = H_0 \hat{z}$, the nuclear spin (assumed to be $S = \frac{1}{2}$) couples as $\mathcal{H} = -\frac{1}{2}\gamma\hbar H_0 \sigma_z$ where γ is the gyromagnetic ratio and σ_z the usual Pauli matrix. The two eigenstates have the usual Zeeman energies, $\pm\frac{1}{2}\hbar\omega_0$, where $\omega_0 = \gamma H_0$ is the Larmor frequency.

For what follows, it will be convenient and later necessary to represent the nuclear spin state in terms of a density matrix ρ . The density matrix ρ represents a quantum state that combines statistical uncertainty with quantum superposition, a *mixed state*. The density matrix $\rho = \sum_m p_m |m\rangle \langle m|$ represents a spin with probability p_m of existing in the eigenstate $|m\rangle$. A more general density matrix will have off-diagonal elements representing superposition between eigenstates, and can be written as $\rho = \sum_{n,m} a_{n,m} |n\rangle \langle m|$. Expectation values for mixed states can be succinctly written $\langle \mathcal{O} \rangle = \text{Tr} \rho \mathcal{O}$, and the Schrodinger equation immediately implies that the den-

sity matrix evolves according to the following Liouville equation $\frac{d\rho}{dt} = \frac{i}{\hbar} [\rho, \mathcal{H}]$. For our Zeeman Hamiltonian, we have the solution $\rho(t) = Z_{\omega_0 t} \rho(0) Z_{\omega_0 t}^{-1}$ where $Z_\theta = e^{-i\frac{\theta}{2}\sigma_z}$ is the spin rotation operator about the z -axis. Likewise, we define X_θ for a rotation about \hat{x} .

Expectation values of magnetic moments, $\langle \vec{\mu} \rangle = \gamma S \hbar \langle \vec{\sigma} \rangle$, are then calculated straightforwardly:

$$\langle \vec{\mu}(t) \rangle = \frac{1}{2} \gamma \hbar \text{tr} \{ \rho(t) \vec{\mu} \} = \frac{1}{2} \gamma \hbar \text{tr} \{ \rho(0) Z_{\omega_0 t}^{-1} \vec{\mu} Z_{\omega_0 t} \} \quad (1)$$

We see that the spin rotation operator Z_θ can be thought of as rotating the magnetic moment an angle θ about the z axis. This is a useful classical picture that accompanies the proper quantum description, and it will be referred to throughout the paper to help visualize the various processes. We see from the above that the external magnetic field causes the magnetic moment to precess about the z -axis at a frequency ω_0 . This precession is a key part of the experiments described in the following section.

Following Rabi, we now introduce an oscillating RF magnetic field $\vec{H}_1 = H_1 (\hat{x} \cos \omega_r t + \hat{y} \sin \omega_r t)$. In order to make its effects more clear, we switch to a co-rotating reference frame. The density matrix in this rotating frame can be related to that in the lab frame according to $\rho_R = Z_{\omega_r t}^{-1} \rho Z_{\omega_r t}$. This state evolves by means of the rotated Hamiltonian

$$\begin{aligned} \mathcal{H}_R &= Z_{\omega_r t}^{-1} \mathcal{H} Z_{\omega_r t} + \frac{\omega_r}{2} \sigma_z \\ &= -\frac{1}{2} \hbar (\omega_0 - \omega_r) \sigma_z - \frac{1}{2} \hbar \omega_1 \sigma_x, \end{aligned} \quad (2)$$

where $\omega_1 = \gamma H_1$.

We are now ready to explain Rabi's result. Suppose our spin is initially in the $+\frac{1}{2}$ eigenstate of S^z . When the RF field is turned off, the spin will be deflected upwards by the Stern-Gerlach apparatus. Now suppose the nucleus is in the presence of the RF field for a time t . If $\omega_r = \omega_0$, then we will have

$$\rho_R(t) = e^{\frac{i}{\hbar} \mathcal{H}_R t} \rho_R(0) e^{-\frac{i}{\hbar} \mathcal{H}_R t} = X(\omega_1 t) \rho_R(0) X^{-1}(\omega_1 t). \quad (3)$$

So our spin is rotated towards the $-\frac{1}{2}$ eigenstate at a frequency ω_1 . This results in an increased fraction of spins being deflected *downwards* by the Stern-Gerlach apparatus rather than upward. On the other hand, if ω_r is far from ω_0 , the RF field has little effect. This is because the

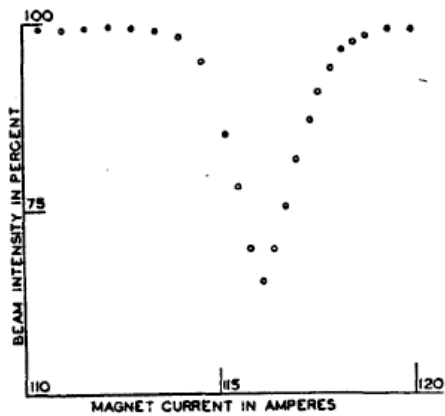


Figure 1 This figure from Rabi’s papers shows the onset of resonance marked by a dip in beam intensity (Rabi *et al.*, 1938).

σ_z term dominates the Hamiltonian and the spin would approximately remain at the $+\frac{1}{2}$ eigenstate. The condition that $\omega_r = \omega_0$ is called the *resonance* condition: the RF field is most effective at flipping the nuclear spin when it oscillates at the Larmour frequency. Hence by varying H_0 until a sudden dip in upwards beam intensity was observed, Rabi was able to determine the nuclear magnetic moment $\gamma = \frac{\omega_r}{H_0}$ (See Fig. 1).

When the RF field is on resonance, we have exquisite control over the nuclear spin state. Starting with a spin in the $+\frac{1}{2}$ eigenstate, we can apply the RF field in strong pulses to tip the spin. For example, applying the field for a time τ_π such that $\omega_1 \tau_\pi = \pi$, we will flip our spin to the $-\frac{1}{2}$ eigenstate. This is called a π -pulse, and it is an essential part of modern NMR experiments. Similarly, we can apply a $\frac{\pi}{2}$ pulse, which puts our spin in an equal superposition of the two eigenstates. In terms of the magnetic moment vectors, a π -pulse rotates the vector from the north pole to the south pole while a $\frac{\pi}{2}$ -pulse rotates it to the equator (See Fig. 3b for a $\frac{\pi}{2}$ -pulse). When the RF field is turned off ($\omega_1 = 0$), Eq. 3 shows that the nuclear state is unchanged in the rotating reference frame, meaning it is precessing about the z -axis in the laboratory frame.

III. NMR of Many Spins - Relaxation

Rabi’s experiment dealt with a beam of non-interacting nuclei, allowing the experiment to be explained in terms of the exactly-solvable dynamics of a single spin in a magnetic field. Modern NMR, on the other hand, deals with large samples containing macroscopic numbers of nuclei. The first experiments of this type were performed in 1946 by Bloch (Bloch *et al.*, 1946) and Purcell (Purcell *et al.*, 1946). Their apparatus consisted of the following main components:

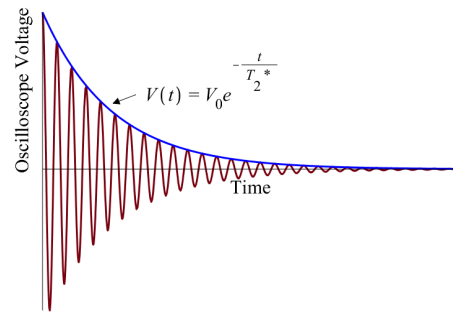


Figure 2 The free induction decay (FID) signal obtained during and NMR experiment with an oscilloscope.

- A homogeneous sample containing a large number of nuclei. Bloch used a vial containing a gram of water, while Purcell used solid wax.
- A strong, uniform magnetic field $H_0 \hat{z}$ across the sample. While these initial experiments used a field strength of fractions of a Tesla, modern experiments often use fields as strong as 21 Tesla created by superconducting magnets.
- A wire coil with an AC current attached to an oscilloscope. This coil supplies the RF magnetic field needed for resonance and also detects the NMR signal.

Similar to Rabi, Bloch and Purcell noticed a sudden absorption of RF radiation when the system was on resonance, indicated by a modulation of the oscilloscope current. Even though the signal from each nucleus would be incredibly small, the large number of nuclei allowed for a measurable voltage.

To explain the elements of this experiment, we consider the modern practice of pulsed NMR developed by both Hahn (Hahn, 1950) and Carr and Purcell (Carr and Purcell, 1954). Here, the RF field is applied in short, strong pulses. The behaviour of the signal between pulses provides key information about the sample. Suppose first that the nuclei are non-interacting. In this case, the spins will initially align along the uniform magnetic field. When the RF field is applied on resonance ($\omega_r = \omega_0$), it will tip the spins according to Eq. 3 causing it to precess about the z -axis. The total magnetization $\vec{M} = \langle \sum_i \vec{\mu}_i \rangle$ will also precess. This precession creates an oscillating magnetic field, which induces an emf in the wire coil according to Faraday’s law. The result AC current would then appear on the oscilloscope as simple sine curve.

In reality, we observe a signal that decays on the order of one second, as pictured in Fig. 2. This signal is known as free induction decay (FID), and analysing its shape forms the basis of all NMR techniques. This decay is due to the fact that our spins are in fact interacting. They interact with neighbouring spins as well as other degrees of freedom such as translational and rotational modes of

molecules in a liquid, or phonons in a solid. Treating these interactions like a perturbation, their net effect is to act as a *thermal bath* for the system. The equilibrium state no longer has all spins aligned with the magnetic field. Rather, the interaction with the bath at temperature T causes each spin to either align or anti-align with the field, with probability given by the Boltzmann weight $e^{-\beta E}$ where E is its Zeeman energy and $\beta^{-1} = k_B T$. This statistical ensemble is the reason we must describe our system in terms of a density matrix.

In equilibrium, the total magnetization satisfies $\vec{M} = M_0 \hat{z}$, so that the transverse components vanish while the longitudinal component reaches a *positive* equilibrium value M_0 . If the magnetization is perturbed from equilibrium, by a RF pulse for example, it will return to equilibrium via the phenomenological Bloch equations (Bloch, 1946):

$$\frac{d\vec{M}}{dt} = \gamma \vec{M} \times \vec{H} - \hat{x} \frac{M_x}{T_2} - \hat{y} \frac{M_y}{T_2} - \hat{z} \frac{(M_z - M_0)}{T_1}. \quad (4)$$

The first term describes the precession of the magnetic moment that we have already derived quantum mechanically. The rest of the terms serve to equilibrate the magnetization. T_1 and T_2 are the longitudinal and transverse relaxations times respectively. Also called the “spin-lattice” and “spin-spin” relaxation times, they give the time scales over which the components of the magnetization equilibrate. T_1 and T_2 are inherent properties of substances like solids, liquids, or solutions, and measuring them provides the means to detect and identify these substances in a laboratory setting. In the next section, we describe how this measurement can be done by analysing the FID signal. Later, we give an outline of how they can be predicted theoretically and which physical processes contribute to the relaxation.

IV. Pulse Sequences

In Section II, we saw that applying the resonant RF field for pulses of varying length can tip the total magnetization of the sample away from equilibrium. These pulses form the basis of the following techniques used to determine T_1 and T_2 . Recall that a θ pulse rotates the magnetization by θ about the x -axis.

A. Measuring T_1 - Inversion Recovery

The sequence of pulses used to measure T_1 can be compactly written $\pi - \tau - \frac{\pi}{2}$. This expresses the following sequence of events known as *inversion recovery*: (1) Apply a π pulse to the sample using the RF coil. (2) Wait for a time τ . (3) Apply a $\frac{\pi}{2}$ pulse and record the initial amplitude of the FID signal. The initial π pulse

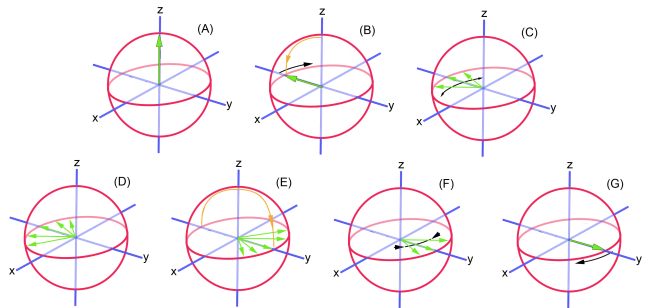


Figure 3 Spin echo viewed in terms of magnetic moments. The initial equilibrium magnetization (a) is rotated by a $\frac{\pi}{2}$ -pulse (b). The moments begin to precess at different rates (c) eventually losing coherence (d). By applying a π -pulse (e), the moments are flipped. The spins precess in the same direction as before, so the decoherence reverses (f) resulting in a spin echo (g) (ech).

serves to flip every spin, inverting the magnetization vector. According to the Bloch equation, the longitudinal magnetization recovers as:

$$M_z(t) = M_0(1 - 2e^{-\frac{t}{T_1}}) \quad (5)$$

However, since the transverse components of the magnetization are still zero, there is no precession and hence no signal. In order to get the signal, the $\frac{\pi}{2}$ pulse is applied to knock the magnetization into the x, y plane. The resulting precession gives a signal whose initial amplitude is proportional to $M_z(\tau)$, as can be verified using Eq. 3.

By repeating this sequence for various values of τ , T_1 can be obtained by fitting the data to simple exponential of Eq. 5. It is important that the system is allowed to equilibrate completely before taking the next data point. Since T_1 can be on the order of seconds, NMR experiments can have significant downtime.

B. Measuring T_2 - Spin Echoes

Suppose our magnetization lies completely in the transverse plane at $t = 0$. According to the Bloch equation, the transverse components will decay as:

$$M_{x,y}(t) = M_{x,y}(0)e^{-\frac{t}{T_2}}. \quad (6)$$

One might think that the FID signal pictured in Fig. 2 can be fit to the above to extract T_2 . After all, it shows the decay of precession in the transverse plane, which is what T_2 is supposed to describe. However, the decay of this signal is due not only to the decay of the transverse magnetization, but also the loss of *coherence* between spins. This decoherence is caused by the fact that each spin i feels a slightly different magnetic field $H_i \neq H_0$ in

the z -direction, so they each precess at a slightly different rate. The greatest contribution to this effect comes from inhomogeneities in the applied magnetic field \vec{H}_0 . Because of this, the transverse magnetization appears to die out prematurely. Therefore the rate of decay of the FID, called T_2^* , is apparatus-dependent, and hence not a good way to classify a sample.

In 1950, Hahn created a technique to solve this problem after observing what he called *spin echoes* (Hahn, 1950). Hahn noticed that, by using the pulse sequence $\frac{\pi}{2} - \tau - \pi$, a sudden revival of the FID signal was observed at a time τ after the π -pulse. To explain this, let's return to the density matrix picture, ignoring interactions for the moment. In the rotating reference frame, the Hamiltonian for spin i reads:

$$\mathcal{H}_{i,R} = -\frac{1}{2}\hbar\delta\omega_i\sigma_z - \frac{1}{2}\hbar\omega_1(t)\sigma_x \quad (7)$$

where the local difference from resonance is $\delta\omega_i = \gamma(H_i - H_0) \ll \omega_1$. We've explicitly shown the time dependence of $H_1(t)$ to be clear that the transverse field is only on for finite durations (pulses). When the pulses are turned off, the evolution operator is $\exp(-\frac{i}{2}\delta\omega_it\sigma_z) = Z_{\delta\omega_it}$, showing that each spin precesses slowly about the z -axis in the rotating frame. During the pulses, the evolution is approximately $\exp(-\frac{i}{2}\omega_1t\sigma_x) = X_{\omega_1t}$ as before. So, with the above pulse sequence, the density matrix $\rho_{i,R}$ for spin i after a time 2τ can be written:

$$\rho_{i,R}(2\tau) = Z_{\delta\omega_i\tau}X_{\pi}Z_{\delta\omega_i\tau}X_{\frac{\pi}{2}}\rho_{i,R}(0)X_{\frac{\pi}{2}}^{-1}Z_{\delta\omega_i\tau}^{-1}X_{\pi}^{-1}Z_{\delta\omega_i\tau}^{-1}.$$

Now we make a remarkable observation. Due to the commutation relations of the Pauli matrices, we can write $Z_{\delta\omega_i\tau}X_{\pi} = X_{\pi}Z_{\delta\omega_i\tau}^{-1}$. This gives the simplification $\rho_{i,R}(2\tau) = X_{\frac{3}{2}\pi}\rho_{i,R}(0)X_{\frac{3}{2}\pi}^{-1}$, showing that every spin undergoes the same evolution, regardless of the local field. That is, the spins regain coherence at time 2τ . We see that by applying the π -pulse, the decoherence of the spins is reversed, giving a resurgence of the FID signal called a spin echo. An explanation in terms of the magnetic moment vectors is given in Fig. 3.

How does this picture change when we bring back interactions? The above demonstration assumed that the local magnetic fields H_i were constant in time. In reality, the interactions cause these fields to rapidly fluctuate, and the decoherence will not be completely undone by the spin echo. These field fluctuations result from fundamental properties of a substance such as molecular structure and mobility. Because of this, the decay in the spin echo amplitude determines T_2 . By repeating the spin echo experiment for different values of τ , Eq. 6 can be fit to obtain T_2 . More sophisticated pulse sequences can be used to eliminate the effects of molecular diffusion, which also contribute to T_2^* (Carr and Purcell, 1954; Meiboom and Gill, 1958).

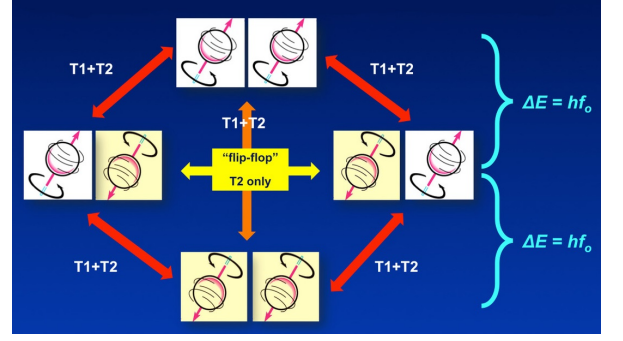


Figure 4 The possible spin interactions cause by the dipole-dipole interaction. Here, $f_0 = \frac{\omega_0}{2\pi}$ (Elster, 1994).

V. Mechanisms of Relaxation

Now that we know how to measure T_1 and T_2 , we show how they can be predicted theoretically. Although this becomes a very difficult problem for complex substances like tissues, it can still be done for systems like water and simple molecular solutions. We begin with some general comments on the nature of the relaxation processes. Firstly, T_1 and T_2 are generally not equal. Since T_1 describes equilibration of the longitudinal magnetization, any process contributing to T_1 must involve a change in energy. This change is caused by spin flips, which are themselves caused by interaction with the bath degrees of freedom. Any spin flip will change the local magnetic fields seen by each spin, so it must also contribute to T_2 as described above. On the other hand, we can have interactions which affect only T_2 , such as a spin “flip-flop” where two spins with opposite orientations suddenly flip with no net energy change. Hence we have $T_1 > T_2$ except in very specialized systems (Traficante, 1991).

To make more observations, we have to consider a specific mechanism of interaction. Here we choose the magnetic dipolar interaction between nuclear spins, which is the dominant effect in spin- $\frac{1}{2}$ nuclei. The dipole-dipole interaction for two spins separated by a vector \vec{r}_{ij} is

$$\mathcal{H}_{ij} = \frac{\gamma^2}{r_{ij}^3} \left(\vec{S}_i \cdot \vec{S}_j - 3(\vec{S}_i \cdot \hat{r}_{ij})(\vec{S}_j \cdot \hat{r}_{ij}) \right). \quad (8)$$

Since the nuclei are not fixed, \vec{r}_{ij} and hence \mathcal{H}_{ij} will be time-dependent. In order to better understand the effects of this equation, we rewrite it as follows (Solomon, 1955):

$$\mathcal{H}_{ij} = F_0 S_i^z S_j^z - \frac{1}{2} F_0 S_i^+ S_j^- + F_1 (S_i^+ S_j^z + S_i^z S_j^+) + F_2 S_i^+ S_j^+ + \text{h.c.} \quad (9)$$

S_i^\pm are the usual spin ladder operators. The lattice functions F_k are time-dependent functions which determine the strength of each term based on the relative position

of the nuclei. F_0 dominates when vector connecting the spins is perpendicular to the magnetic field, F_2 dominates when it is parallel, and F_1 dominates in between. We see that the dipole-dipole interaction has various interaction channels that can leave both spins unchanged, flip one of them, or flip both. This is illustrated in Fig. 4. $F_{\Delta m}$ is labelled to correspond to spin interactions that change the total spin by Δm .

To see how this interaction contributes to T_1 and T_2 , one can employ what is known as Redfield theory (Redfield, 1957). This technique describes the evolution of two spins in the presence of the thermal bath. It is essentially second order perturbation theory, with the addition that the vector \vec{r}_{ij} connecting the spins is a stochastic variable due to the interactions with the bath. By taking a thermal average over \vec{r}_{ij} , one can obtain a master equation describing the evolution of the two spins. This can be used to determine the evolution of the magnetic moments of each pair of spins, which gives in turn the total magnetization. The results of this calculation are (Solomon, 1955; Abragam, 1961):

$$T_1^{-1} = \frac{9}{4}\gamma^4\hbar^2[J_1(\omega_0) + \frac{1}{2}J_2(2\omega_0)], \quad (10)$$

$$T_2^{-1} = \frac{9}{4}\gamma^4\hbar^2 \left[\frac{1}{4}J_0(0) + \frac{5}{2}J_1(\omega_0) + \frac{1}{4}J_2(2\omega_0) \right]. \quad (11)$$

The functions $J_{\Delta m}(\omega)$ are obtained by Fourier transforming thermal correlation functions of $F_{\Delta m}$; the so-called *spectral density functions*. Loosely, they encode the intensity at which the lattice functions $F_{\Delta m}$ fluctuate at frequency ω due to interactions with the bath. We notice $J_{\Delta m}(\omega)$ appears in the above only at $\omega = \Delta m\omega_0$. This is expected: $F_{\Delta m}$ is connected with interactions that change the total spin by Δm and require an exchange of energy $\hbar\Delta m\omega_0$. Hence the amount $F_{\Delta m}$ fluctuates at frequency $\Delta m\omega_0$ is most important for transitions.

Notice that both T_1 and T_2 depend on $J_1(\omega)$ and $J_2(\omega)$. These are thermalizing channels that involve exchange of energy with the bath, so this is consistent with our above discussion. However the zero-mode $J_0(0)$, describing the static part of the fluctuations, appears only in T_2 . This is because this channel involves no exchange of energy, and it in fact corresponds to the spin flip-flop.

Similar equations can be derived for different kinds of interactions. For nuclei of spin greater than $\frac{1}{2}$, electric quadrupole radiation is the dominant interaction. For more complex substances, intermolecular interactions between nuclei can be mediated by the electrons, causing the so-called J -coupling. Often, it is too difficult to accurately predict the relaxation times, and they must be obtained experimentally.

VI. Conclusion - Applications of NMR

We conclude with a brief mention of some of the modern applications of NMR. As described in the beginning, NMR provides a simple mechanism to measure the nuclear magnetic moment. However, by applying more sophisticated pulse sequences, the same principles can be used to obtain much more information.

The most common application of NMR is magnetic resonance imaging (MRI) (Haacke *et al.*, 1999). Here, images of a human body are created from the T_1 and T_2 properties of the composing tissues. By applying magnetic fields with gradients, the RF field will resonate with only specific sections of the body. The nuclei involved in resonance typically come from molecules of either fat or water. Water, due to its relative lack of internal degrees of freedom, has a long T_1 . Fatty acids, on the other hand, contain complex rotation and flexing modes that can often be near the Larmor frequency, providing the means for T_1 relaxation. Hence, by mapping the value of T_1 throughout a section of the body, an image can be formed. Similarly, we can make T_2 -weighted images, and many more variations to get a comprehensive picture.

A second key example is NMR spectroscopy (Breitmaier and Voelter, 1987). Here, the main source of information is the Fourier transformation of the FID signal. When a complex molecule is in solution, each nucleus in the molecule will feel a slightly different local magnetic field due to the other atoms. This phenomenon, known as the chemical shift, makes each nucleus precess at a different rate, appearing as peaks on the Fourier transform of the FID. Further information can be obtained by the number of peaks at a given frequency: the aforementioned J -coupling causes peaks to split into multiplets when a molecule contains identical nuclei. These effects, among others, allow us to extract not only the type of nuclei present in a sample molecule, but also the number.

Finally, NMR has found use in the field of quantum computation (Vandersypen and Chuang, 2005). Atoms in a molecule with different resonant frequencies due to the chemical shift can be controlled individually by the RF field. This allows them to act as distinct quantum bits (qubits) Applying a π -pulse to a single atom is equivalent to a logical “X” operation (quantum NOT), and other pulse sequences give the rest of the single-qubit operations. By taking advantage of the J -coupling, different qubits can even be entangled. Of course, an NMR sample contains many interacting molecules which will serve to destroy the logical information. But the system will remain coherent as long as operations are done on a time scale much shorter than T_1 or T_2 , and this has been demonstrated by implemented the coveted Shor’s factoring algorithm on an NMR quantum computer (Vandersypen *et al.*, 2001).

References

- I. I. Rabi, J. R. Zacharias, S. Millman, and P. Kusch, *Phys. Rev.* **53**, 318 (1938).
- F. Bloch, W. W. Hansen, and M. Packard, *Phys. Rev.* **69**, 127 (1946).
- E. M. Purcell, H. C. Torrey, and R. V. Pound, *Phys. Rev.* **69**, 37 (1946).
- E. L. Hahn, *Phys. Rev.* **80**, 580 (1950).
- H. Y. Carr and E. M. Purcell, *Phys. Rev.* **94**, 630 (1954).
- F. Bloch, *Phys. Rev.* **70**, 460 (1946).
- “G-7a pulsed nmr : Spin echo,” http://pages.physics.cornell.edu/p510/G-7A_Pulsed_NMR:_Spin_Echo, accessed: 2016-11-25.
- S. Meiboom and D. Gill, *Review of scientific instruments* **29**, 688 (1958).
- A. D. Elster, “Questions and answers in magnetic resonance imaging. st. louis: Mosby-year book,” (1994).
- D. D. Traficante, *Concepts in Magnetic Resonance* **3**, 171 (1991).
- I. Solomon, *Phys. Rev.* **99**, 559 (1955).
- A. G. Redfield, *IBM Journal of Research and Development* **1**, 19 (1957).
- A. Abragam, *The principles of nuclear magnetism*, 32 (Oxford university press, 1961).
- E. M. Haacke, R. W. Brown, M. R. Thompson, R. Venkatesan, et al., *Magnetic resonance imaging: physical principles and sequence design*, Vol. 82 (Wiley-Liss New York:, 1999).
- E. Breitmaier and W. Voelter, (1987).
- L. M. Vandersypen and I. L. Chuang, *Reviews of modern physics* **76**, 1037 (2005).
- L. M. Vandersypen, M. Steffen, G. Breyta, C. S. Yannoni, M. H. Sherwood, and I. L. Chuang, *Nature* **414**, 883 (2001).